

The formation of direct collapse black holes under the influence of streaming velocities

Anna T. P. Schauer^{1*}, John Regan^{2,1}, Simon C. O. Glover¹, Ralf S. Klessen^{1,3}

¹ *Universität Heidelberg, Zentrum für Astronomie, Institut für Theoretische Astrophysik, Albert-Ueberle-Str. 2, 69120 Heidelberg, Germany*

² *Centre for Astrophysics & Relativity, School of Mathematical Sciences, Dublin City University, Glasnevin, D09 W6Y4, Dublin, Ireland*

³ *Universität Heidelberg, Interdisziplinäres Zentrum für Wissenschaftliches Rechnen, Im Neuenheimer Feld 205, 69120 Heidelberg, Germany*

28 July 2021

ABSTRACT

We study the influence of a high baryonic streaming velocity on the formation of direct collapse black holes (DCBHs) with the help of cosmological simulations carried out using the moving mesh code AREPO. We show that a streaming velocity that is as large as three times the root-mean-squared value is effective at suppressing the formation of H_2 -cooled minihaloes, while still allowing larger atomic cooling haloes (ACHs) to form. We find that enough H_2 forms in the centre of these ACHs to effectively cool the gas, demonstrating that a high streaming velocity by itself cannot produce the conditions required for DCBH formation. However, we argue that high streaming velocity regions do provide an ideal environment for the formation of DCBHs in close pairs of ACHs (the “synchronised halo” model). Due to the absence of star formation in minihaloes, the gas remains chemically pristine until the ACHs form. If two such haloes form with only a small separation in time and space, then the one forming stars earlier can provide enough ultraviolet radiation to suppress H_2 cooling in the other, allowing it to collapse to form a DCBH. Baryonic streaming may therefore play a crucial role in the formation of the seeds of the highest redshift quasars.

Key words: black hole physics – stars: Population III – (cosmology:) early Universe – (galaxies:) quasars: supermassive black holes.

1 INTRODUCTION

Massive black hole seeds that can form through gravitational collapse of very massive progenitors, (Chandrasekhar 1964), can be invoked to explain the observations of quasars at very early times in the Universe (Wu et al. 2015; Mortlock et al. 2011; Fan et al. 2006). The direct collapse (DC) model (Loeb & Rasio 1994; Oh & Haiman 2002; Bromm & Loeb 2003; Begelman, Volonteri & Rees 2006; Regan & Haehnelt 2009a,b) of super-massive black hole (SMBH) formation requires that massive objects form in near pristine atomic cooling haloes in which Population III (Pop III) star formation has been suppressed. The suppression of previous episodes of star formation means that metal enrichment is obviated. Pop III star formation can be restrained by removing the primary gas coolant, H_2 , or alternatively by increasing the minimum halo mass required for collapse due to the impact of streaming motions as we shall see.

One avenue that has been explored by many authors to suppress H_2 formation is radiative feedback from the sur-

rounding galaxies in the Lyman-Werner (LW) band (Shang, Bryan & Haiman 2010; Agarwal et al. 2012; Regan, Johansson & Wise 2014; Latif et al. 2014a; Agarwal et al. 2014; Agarwal & Khochfar 2015; Hartwig et al. 2015; Regan, Johansson & Wise 2016a). LW radiation readily dissociates H_2 through the two step Solomon process (Field, Somerville & Dressler 1966; Stecher & Williams 1967). For high star formation efficiencies or single, massive Pop III stars, most of the LW radiation can escape the host galaxy or minihalo (Schauer et al. 2015, 2017). If the intensity of the LW radiation is sufficient, H_2 is dissociated and cooling is suppressed in low mass minihaloes. The halo then continues to accrete mass all the way up to and beyond the atomic line cooling limit. Halo collapse can then begin once Lyman- α line cooling becomes effective and contraction proceeds isothermally at approximately $T_{\text{gas}} \sim 8000$ K. In this case, the strength of the background required depends both on the spectral shape of the sources and on their proximity with respect to the target halo (Dijkstra et al. 2008; Sugimura, Omukai & Inoue 2014; Agarwal et al. 2016). There is general consensus within the literature that the critical value of the background required to suppress H_2 formation throughout the entire halo

* E-mail:schauer@uni-heidelberg.de

is $J_{\text{crit}} \sim 1000 J_{21}$ for a background dominated by emission from stars with an effective temperature $T_{\text{eff}} \sim 5 \times 10^4$ K, where $J_{21} = 10^{-21} \text{ erg cm}^{-2} \text{ s}^{-1} \text{ Hz}^{-1} \text{ sr}^{-1}$. If there is also a non-negligible X-ray background, then the required value can be even higher (Inayoshi & Tanaka 2015; Glover 2016; Regan, Johansson & Wise 2016b). A much milder intensity level, say $J \lesssim 100 J_{21}$, is enough to delay Pop III formation until a halo reaches the atomic cooling limit, but in this case H_2 readily forms in the self-shielded core of the ACH, resulting in rapid Pop III formation (e.g. Fernandez et al. 2014; Regan et al. 2017).

The value of J_{crit} is orders of magnitude higher than the typical strength of the Lyman-Werner background at the relevant redshifts, even if one accounts for clustering of sources (Ahn et al. 2009). Radiation fields of the required strength will therefore only be encountered in unusual circumstances. One promising way in which a field of the required strength can be produced is the synchronised halo model (Dijkstra et al. 2008; Visbal, Haiman & Bryan 2014b; Regan et al. 2017; Agarwal et al. 2017). This model supposes that occasionally two ACHs will be found in close proximity. If both haloes remain chemically pristine until the onset of atomic cooling, and if the collapse times of the haloes are sufficiently similar, then Pop III star formation can begin in the first halo before the second has finished collapsing. The resulting irradiation from the more evolved system provides a sufficiently strong LW radiation field to suppress cooling in the secondary (proto-)galaxy, which therefore becomes an ideal location for the formation of a DCBH. However, for this model to work, it is necessary to suppress H_2 formation in both haloes until they become massive enough to atomically cool. If this is accomplished via LW feedback, the required field strength is $J \gtrsim 100 J_{21}$, which is still somewhat higher than the typical strength of the LW background.

Another, perhaps more natural, mechanism for delaying Pop III star formation is via streaming of the baryons with respect to the dark matter. This effect, elucidated by Tselikhovich & Hirata (2010), is a result of the initial offset between the baryonic velocities and the dark matter velocities after recombination. The velocity offset between baryons and dark matter decays as $\Delta v \propto (1+z)$, but offsets as large as 9 km s^{-1} are still possible at $z \sim 100$. The impact of this streaming motion on Pop III star formation have been investigated by several authors with general agreement that the minimum halo mass required for Pop III star formation is increased in the presence of large-scale streaming velocities (Stacy, Bromm & Loeb 2011; Greif et al. 2011; Naoz, Yoshida & Gnedin 2013, Schauer et al. 2017b in prep) as the baryons require a larger gravitational potential in which they can virialise due to the additional streaming velocity. Therefore, streaming motions are not thought to have a large effect on ACHs illuminated with LW radiation fields with strengths greater than J_{crit} (i.e. haloes which would form DCBHs even without the streaming; see Latif, Niemeyer & Schleicher 2014 for details). However, Tanaka & Li (2014) argue that very large streaming velocities may suppress Pop III star formation entirely in some haloes, allowing pristine haloes above the atomic cooling limit to form, thereby providing ideal locations in which DCBHs can form without requiring an extremely strong LW radiation field. This model has been criticised by Visbal, Haiman & Bryan (2014a), who concede that streaming can suppress H_2 formation in mini-

haloes but argue that in ACHs, H_2 formation in dense collapsing gas is inevitable, regardless of the streaming velocity, unless the gas is illuminated by a strong LW radiation field. Other models which can successfully suppress H_2 cooling and delay PopIII formation have been put forward by Inayoshi & Omukai (2012) (collisional dissociation by shocks), Fernandez et al. (2014) (rapid accretion in a mild LW background) and Inayoshi, Visbal & Kashiyama (2015) (proto-galactic collisions) among other. However, here we focus on streaming velocities as a mechanism for increasing the minimum mass for star formation and hence for creating ideal environments for DCBH formation.

In this paper, we re-examine the role of baryonic streaming in the formation of DCBHs. We show that although baryonic streaming by itself cannot produce haloes capable of forming DCBHs, it provides a very natural mechanism for suppressing H_2 formation in pairs of haloes until they reach the atomic cooling regime. It therefore offers a simple way of producing the pristine ACH pairs required by the synchronised halo model without the need for a locally elevated LW background. Furthermore, the risk of metal enrichment from background galaxies is significantly reduced since mini-halo formation is suppressed in the immediate vicinity.

2 SIMULATIONS

2.1 Numerical method

The simulations described in this paper are carried out using the AREPO moving-mesh code (Springel 2010). We include both dark matter particles and gas cells. The hydrodynamics of the gas is evolved using a Voronoi grid in which the gas cells move along with the flow. We use a recent version of AREPO that includes improvements to the time integration scheme, spatial gradient reconstruction and grid regularization discussed in Pakmor et al. (2016) and Mocz et al. (2015). We model the thermal and chemical evolution of the gas in our cosmological boxes using an updated version of the chemical network and cooling function implemented in AREPO by Hartwig et al. (2015), based on earlier work by Glover & Jappsen (2007) and Clark et al. (2011). Our chemical model accounts for the formation of H_2 by the H^- and H_2^+ pathways and its destruction by collisions and by photodissociation. It includes all of the chemical reactions identified by Glover (2015) as being important for accurately tracking the H_2 abundance in simulations of DCBH formation.

Compared to Hartwig et al. (2015), we have made three significant changes to the chemical network. First, we have included a simplified treatment of deuterium chemistry designed to track the formation and destruction of HD following Clark et al. (2011). Second, we have updated the rate coefficient used for the dielectronic recombination of ionized helium, He^+ ; we now use the rate calculated by Badnell (2006). Finally, we have improved our treatment of H^- photodetachment to account for the contribution to the H^- photodetachment rate coming from non-thermal CMB photons produced as a consequence of cosmological recombination (Hirata & Padmanabhan 2006). We describe this process using the simple analytical expression given in Coppola et al. (2011).

Name	Box length (h^{-1} Mpc)	M_{DM} (M_{\odot})	$M_{\text{gas,init}}$ (M_{\odot})
SB	1	99	18.6
LB	4	6360	1190

Table 1. Dark matter particle mass and initial mesh cell gas mass in our two simulations.

Our treatment of the cooling accounts for all of the processes important at the number densities probed by our simulations, including Lyman- α cooling and H₂ rotational and vibrational cooling. The latter is taken from Glover & Abel (2008) and updated as described in Glover (2015). Further details of our chemical and thermal treatment can be found in Schauer et al. (2017, in prep).

2.2 Initial conditions

We initialise our simulations at $z = 200$. We assume a Λ CDM cosmology and use cosmological parameters from the 2015 Planck data release (Planck Collaboration et al. 2016). Unless we explicitly state otherwise, we use physical units throughout the paper. The initial conditions for the dark matter are created with MUSIC (Hahn & Abel 2011), using the transfer functions of Eisenstein & Hu (1998). The baryons are assumed to initially trace the dark matter density distribution. To account for the supersonic streaming of the baryons relative to the dark matter, we first set up a velocity field in the baryonic component that is the same as that in the dark matter, and then impose a constant velocity offset, v_{stream} . We take the magnitude of this offset to be $v_{\text{stream}} = 18 \text{ km s}^{-1}$ at $z = 200$, corresponding to a value of $3 \sigma_{\text{rms}}$, of the root-mean-squared streaming velocity at this redshift (Tsaliakhovich & Hirata 2010).

We carry out two simulations, runs SB (small box) and LB (large box). In run SB, we model a box of size (1 Mpc/ h) in comoving units, while in run LB, we consider a box of size (4 Mpc/ h). Both simulations are performed using 1024^3 dark matter particles and initially represent the gas using 1024^3 Voronoi mesh cells. In run SB, we therefore have a dark matter particle mass of $99.4 M_{\odot}$ and an average initial mesh cell mass of $18.6 M_{\odot}$. In run LB, these values are a factor of 64 larger, as summarised in Table 1. If we conservatively require 1000 dark matter particles in order to consider a halo to be resolved (Sasaki et al. 2014, Schauer et al. 2017b in prep.), then the corresponding resolution limits are $M_{\text{DM,res}} \simeq 10^5 M_{\odot}$ for run SB and $M_{\text{DM,res}} \simeq 6.4 \times 10^6 M_{\odot}$ for run LB. We note that even in our lower resolution, larger box run, the minimum resolvable halo mass is smaller than the minimum mass of an ACH in the range of redshifts considered in this paper, $M_{\text{atom}} \sim 10^7 M_{\odot}$.

For gas number densities $n < 100 \text{ cm}^{-3}$, we adopt a ‘‘constant mass’’ refinement criterion, meaning that AREPO refines or de-refines mesh cells as required in order to keep the mass of gas in each cell at its initial value, plus or minus some small tolerance. At $n \geq 100 \text{ cm}^{-3}$, we instead use Jeans refinement, and ensure that the Jeans length is always resolved by at least eight mesh cells. However, in order to prevent run-away collapse to protostellar densities, we switch off refinement once the cell volume becomes less than

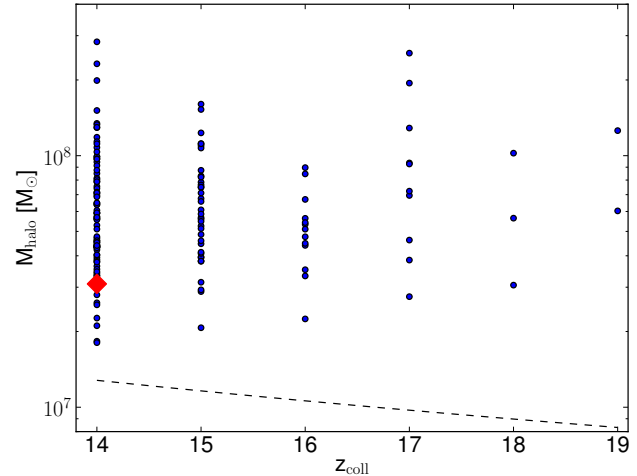


Figure 1. Masses of haloes containing cold dense gas, plotted at their redshift of collapse z_{coll} , defined as described in Section 3. The clustering of points at particular values of z_{coll} reflects the fact that we produce output snapshots with a redshift separation $\Delta z = 1$. The red diamond denotes the halo in simulation SB, and the blue circles denote the haloes in simulation LB. All collapsed haloes have masses larger than the minimum mass of an ACH (denoted by the dashed black line), demonstrating that only ACHs can collapse when $v_{\text{stream}} = 3\sigma_{\text{rms}}$.

$0.1 h^{-3} \text{ pc}^3$ in comoving units, corresponding to a density of $n \sim 10^6 \text{ cm}^{-3}$.

3 RESULTS

3.1 Masses and collapse redshifts of haloes containing cold dense gas

We expect runaway collapse for densities exceeding a number density of $n \geq 10^4 \text{ cm}^{-3}$ (Glover 2005). We therefore call a halo collapsed when this number density is exceeded by at least one gas cell in that halo. In our simulations, the first objects collapse at $z = 19$ in simulation LB and at $z = 14$ in simulation SB. This difference in collapse redshift is an expected consequence of the difference in box size: simulation LB contains more large-scale power and hence naturally forms collapsed objects somewhat earlier than simulation SB.

In Figure 1, we show the halo mass at collapse as a function of collapse redshift z_{coll} . In our simulations, we produce output snapshots with a redshift spacing $\Delta z = 1$ in order to restrict the volume of data produced to a reasonable level. We can therefore not distinguish between haloes forming at e.g. $z = 19.99$ and $z = 19.01$, leading to the clear clustering of points in the Figure.

In simulation SB, we form only a single collapsed halo by the end of the simulation. This object has a mass of $3 \times 10^7 M_{\odot}$ and a collapse redshift $z_{\text{coll}} = 14$. In run LB, on the other hand, the larger box allows us to form more collapsed haloes. We find 2, 3, 10, 13, 37 and 86 haloes that collapse at redshifts $z = 19, 18, 17, 16, 15$ and 14, respectively. In every single case, the halo mass at collapse is larger than the mass of a halo with a virial temperature of 8000 K (indicated by the dashed black line in Figure 1), which is a reasonable

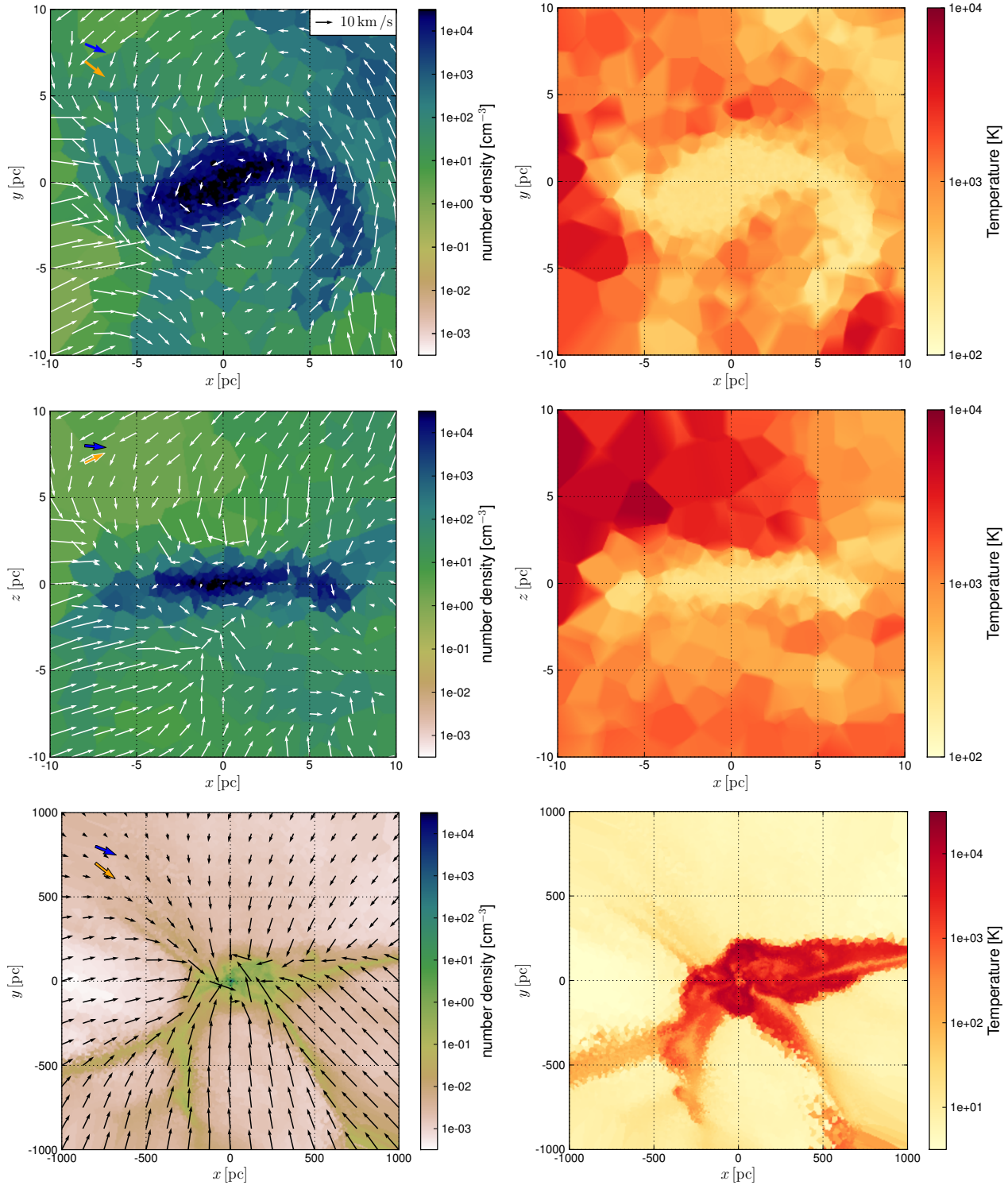


Figure 2. Number density (left panels) and temperature (right panels) slices of the collapsed halo with $M_{\text{halo}} = 3 \times 10^7 M_{\odot}$ in the SB simulation at redshift $z = 14$. In the upper two rows, we show the central region in face-on and edge-on projections. In the bottom row, we show the larger-scale structure surrounding the halo. The distances shown are in proper units. The black or white arrows in the density slices show the velocity field of the closest cell projected into the plane. (Note that the velocities shown are computed in the centre of mass rest-frame.) In blue, we show the streaming velocity at this redshift, scaled up by a factor of 10, and in orange the velocity of the centre of mass. We can see that the centre of the halo is dense and cold with temperatures around a few hundred K. This is the place where Pop III star formation will eventually take place. On larger scales, the gas flows that feed the halo are visible.

proxy for the minimum mass of an ACH. Previous work has shown that Pop III stars in regions of the Universe with no streaming velocity can form in minihaloes with masses of a few times $10^5 M_{\odot}$ (Machacek, Bryan & Abel 2001; Yoshida et al. 2003; Hirano et al. 2015). We find no cold dense gas in any halo with a mass less than the atomic cooling limit, demonstrating that when the baryonic streaming velocity is very high, the formation of Pop III stars in H_2 -cooled minihaloes is very strongly suppressed.

Our results demonstrate that high baryonic streaming velocities are a viable mechanism for producing a population of chemically pristine ACHs without the need for a high LW background. A sufficient close pair of such haloes collapsing at very similar redshifts would be an ideal site for the formation of a DCBH (Visbal, Haiman & Bryan 2014b; Regan et al. 2017). We have carefully examined whether any of the collapsed haloes in the LB simulation have separations of less than 500 pc in proper units, which is a reasonable upper limit on the required separation, but have found no such close pairs. However, this is unsurprising, since their space density is expected to be very small. In their simulations, Visbal, Haiman & Bryan (2014b) find two closely synchronized halo pairs in a volume of $\approx 1.7 \times 10^4 \text{ cMpc}^3$, corresponding to a number density of $1.2 \times 10^{-4} \text{ cMpc}^{-3}$, where cMpc denotes comoving Mpc. Since the combined volume of simulations SB and LB is much smaller (209 cMpc^3), the probability of finding a synchronized pair is only $\sim 2.5\%$.

The fraction of the Universe with streaming velocities of $3\sigma_{\text{rms}}$ or higher is $\approx 5.9 \times 10^{-6}$. If we assume that all high-redshift quasars originate from synchronized halo pairs in regions with $v_{\text{stream}} \geq 3\sigma_{\text{rms}}$, then we find a quasar number density of 0.7 cGpc^{-3} . This number is in good agreement with the low number density of quasars observed at redshift $z = 6$ of about 1 cGpc^{-3} (Fan 2006). This statement is based on the assumption that all observed high-redshift quasars can be well observed and are not quiescent or hidden in a dust cloud. Thus the real number density of quasars could be higher than the value that is observed today.

3.2 Gas properties within the collapsed haloes

Next, we take a closer look at the collapsed halo in simulation SB. In Figure 2, we show slices of the number density and the temperature of the central region and the surroundings of our halo at redshift $z = 14$. In the upper left panel, we see the face-on cut-through of the central 20 pc, where all of the dense, collapsed gas can be found. Here, the densities are high enough for efficient formation of H_2 , leading to strong cooling. The dense region thus corresponds to a region of low temperature (upper right panel). In the edge-on cut-through (middle left and middle right panels), one can see a stream of hot, low-density gas flowing onto the halo. The larger-scale structure in which the halo is embedded can be seen in the lower two panels. It is in the middle of several hot gas streams that feed the minihalo. The central 200 pc region is shock-heated up to 10^4 K , except for some high-density streams that already cool efficiently.

In Figure 3, we can see the radial profiles of our halo in the SB simulation. As can already be seen from the slice plots in Figure 2, we see a drop in temperature at the centre of the halo, corresponding to a region of high density and high H_2 abundance. Furthermore, in the bottom

right hand panel of Figure 3 we see that the mass inflow rate onto the central region is, on average, well below the threshold value of $\sim 0.1 M_{\odot} \text{ yr}^{-1}$ for forming supermassive stars (e.g. Hosokawa et al. 2013; Schleicher et al. 2013). These results confirm the argument put forward by Visbal, Haiman & Bryan (2014a) that high streaming velocities are unable to prevent H_2 formation in dense gas in ACHs, and demonstrate that the suggestion of Tanaka & Li (2014) that streaming velocities alone can create the necessary conditions for DCBH formation is incorrect.

In the top panel of Figure 4, we show a two-dimensional histogram of all gas cells in simulation LB in a $\log(n)$ - $\log(T)$ diagram. The region with low number density and temperature corresponds to void regions in the simulation, where the gas can cool below the CMB temperature adiabatically. In the bottom panel of Figure 4, we depict the same histogram, but only for gas cells associated with the collapsed haloes at this redshift. Unsurprisingly, there are no cells in the low density, low temperature regime.

Above gas number densities of $n > 1 \text{ cm}^{-3}$, most of the gas undergoes cooling and settles into temperatures of a few hundred K. There is, however, some gas that occupies the high density, high temperature region in the diagram. We carefully check that this hot ($T > 4000 \text{ K}$), dense ($n > 10^4 \text{ cm}^{-3}$) gas can be traced back to shock heating of individual cells in the haloes (as predicted by Inayoshi & Omukai 2012). These cells are typically located at the edge of the high density, cold centre of the halo, where it is intersected by an inflowing gas stream (compare with Latif et al. 2014b, who find a similar behaviour in their low LW halo). In the bottom panel of Figure 4 we see that the majority of the dense, collapsed gas in our haloes cools efficiently via H_2 and HD emission down to temperatures of around a hundred K. We can therefore safely conclude that all of the collapsed haloes that form in our simulations have a cold, dense centre, and are therefore unlikely to collapse to form DCBHs in the absence of external LW feedback.

4 CONCLUSIONS

In this paper, we have investigated the role that high baryonic streaming velocities may play in the formation of DCBHs. We carried out two simulations in which we imposed a constant velocity offset, $v_{\text{stream}} = 3\sigma_{\text{rms}}$, where σ_{rms} is the root-mean-squared streaming velocity. One of these simulations used a volume of side length $1 \text{ cMpc}/h$, giving us very good mass resolution, but producing only a single sample of an ACH. The other simulation used a larger volume with side length $4 \text{ cMpc}/h$, and consequently had worse mass resolution but yielded a much larger sample of ACHs. In both cases, we find that the effect of the large streaming velocity is to suppress H_2 formation (and hence star formation) in minihaloes: the first haloes in which gas is able to cool and collapse to high densities are all ACHs. However, contrary to a suggestion by Tanaka & Li (2014), we find no evidence for the suppression of H_2 cooling in any of the collapsed ACHs. In every case, H_2 forms within the centre of the halo, and so in the absence of additional physics, we would expect all of the haloes to form Pop III stars rather than DCBHs. In the cases where Pop III star formation is the final result and if the Pop III star(s) find themselves at

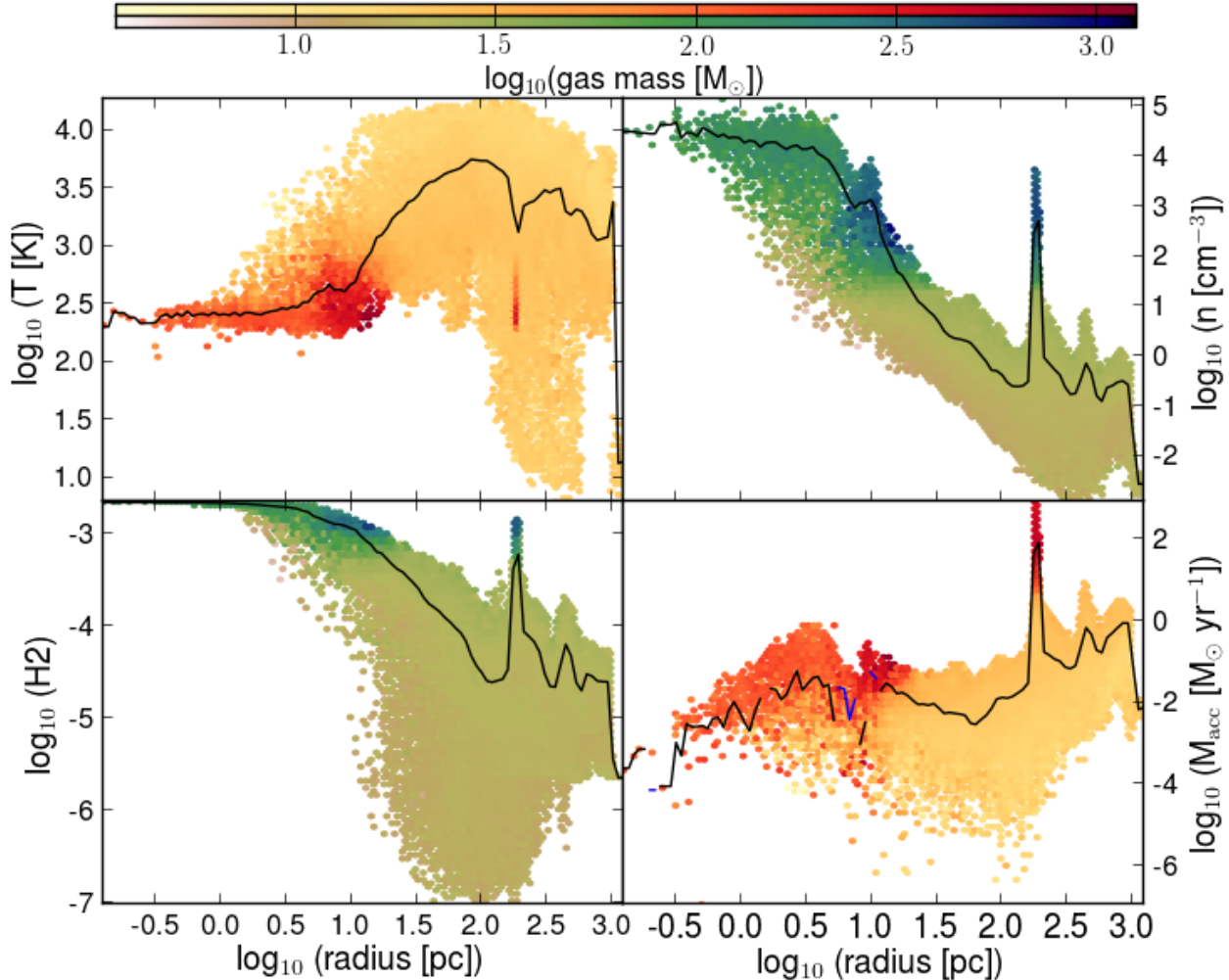


Figure 3. Properties of the collapsed halo with $M_{\text{halo}} = 3 \times 10^7 M_{\odot}$ in the SB simulation at redshift $z = 14$. From top left to bottom right, we show the temperature, gas number density, H_2 abundance and mass accretion rate as a function of radius, with the radius given in proper units. The colored regions show two dimensional histograms of the distribution of gas cells, the black lines the mass averaged values. For the mass accretion rate, we show a blue line for outflowing masses. In the central, high density halo region, the temperature drops to a few hundred Kelvin due to cooling by H_2 . In the same region, the H_2 abundance reaches values above 10^{-3} . Since the accretion rate is low ($\approx 10^{-2} M_{\odot} \text{ yr}^{-1}$), we expect Pop III star formation and not the formation of a supermassive star that eventually collapses into a DCBH.

the centre of a convergent flow with high in-fall rates then rapid growth may be possible even when starting from a so-called “lighter seed” (Lupi et al. 2016; Pezzulli, Valiante & Schneider 2016).

Nonetheless, our results demonstrate that high streaming velocities cannot by themselves produce the conditions required for DCBH formation. However, they do produce an ideal environment in which the synchronised halo model for DCBH formation can operate. This model requires that star formation be suppressed in a close pair of haloes until both reach masses large enough that they can start to atomically cool (Dijkstra et al. 2008; Visbal, Haiman & Bryan 2014b; Regan et al. 2017). Achieving this with LW feedback is possible, but requires a LW radiation field strength that is significantly higher than the typical background value (Visbal, Haiman & Bryan 2014b). High streaming velocities provide an alternative means of achieving the same suppression without the need for a locally elevated LW background, and

without the risk that the haloes will be enriched with metals from nearby minihaloes. In addition, if we estimate the comoving number density of synchronised halo pairs that are located in regions with $v_{\text{stream}} \geq 3\sigma_{\text{rms}}$, we find a number of order 1 cGpc^{-3} , in good agreement with the observed comoving number density of $z > 6$ quasars. We conclude that synchronised halo pairs forming in regions of very high baryonic streaming velocity are ideal candidates for forming the seeds of the first quasars.

ACKNOWLEDGMENTS

The authors would like to acknowledge fruitful discussions with Naoki Yoshida and Takashi Hosokawa as well as with Mattis Magg and Mattia Sormani. They would like to thank the anonymous referee for her/his valuable comments that helped to improve the paper. ATPS would like to thank

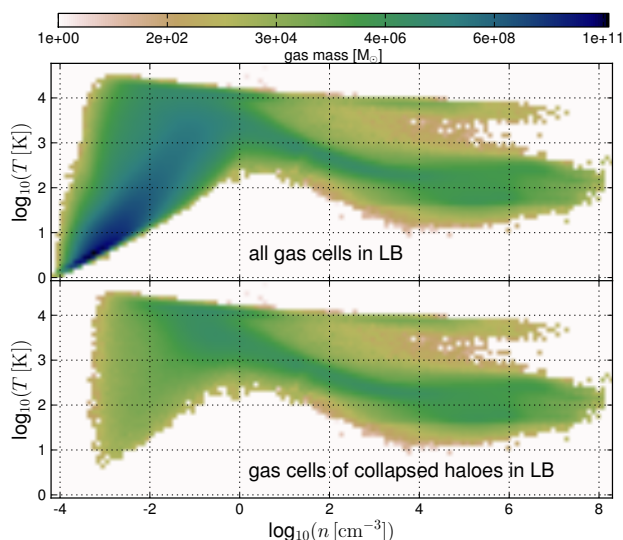


Figure 4. Two dimensional histograms of all gas cells in $\log(n)$ – $\log(T)$ space at redshift $z = 14$. The upper panel shows all gas cells in simulation LB, the lower panel all gas cells in LB that are associated with the collapsed haloes. Above number densities of $n \gtrsim 1 \text{ cm}^{-3}$, the majority of the gas cells under-go cooling by H_2 and HD and reach temperatures as low as hundred K. The few high density – high temperature gas cells can be associated with single shocked gas cells in some haloes. We can conclude that all collapsed haloes in simulation LB have cool, dense centres similar to the halo in simulation SB.

Volker Springel and his team for kindly providing the code AREPO that was used to carry out this simulation. Special thanks goes to Christian Arnold, Rüdiger Pakmor, Kevin Schaal, Christine Simpson and Rainer Weinberger for their help with the code. ATPS, SCOG and RSK acknowledge support from the European Research Council under the European Community’s Seventh Framework Programme (FP7/2007 - 2013) via the ERC Advanced Grant “STARLIGHT: Formation of the First Stars” (project number 339177). SCOG and RSK also acknowledge support from the Deutsche Forschungsgemeinschaft via SFB 881 “The Milky Way System” (sub-projects B1, B2 and B8) and SPP 1573 “Physics of the Interstellar Medium” (grant number GL 668/2-1). JR acknowledges the support of the EU Commission through the Marie Skłodowska-Curie Grant - “SMARTSTARS” - grant number 699941. The authors gratefully acknowledge the Gauss Centre for Supercomputing e.V. (www.gauss-centre.eu) for funding this project by providing computing time on the GCS Supercomputer SuperMUC at Leibniz Supercomputing Centre (www.lrz.de). The authors acknowledge support by the state of Baden-Württemberg through bwHPC and the German Research Foundation (DFG) through grant INST 35/1134-1 FUGG.

REFERENCES

Agarwal B., Dalla Vecchia C., Johnson J. L., Khochfar S., Paardekooper J.-P., 2014, MNRAS, 443, 648
 Agarwal B., Khochfar S., 2015, MNRAS, 446, 160
 Agarwal B., Khochfar S., Johnson J. L., Neistein E., Dalla Vecchia C., Livio M., 2012, MNRAS, 425, 2854

Agarwal B., Regan J., Klessen R. S., Downes T. P., Zackrisson E., 2017, MNRAS, submitted; arXiv:1703.08181
 Agarwal B., Smith B., Glover S., Natarajan P., Khochfar S., 2016, MNRAS, 459, 4209
 Ahn K., Shapiro P. R., Iliev I. T., Mellema G., Pen U., 2009, ApJ, 695, 1430
 Badnell N. R., 2006, A&A, 447, 389
 Begelman M. C., Volonteri M., Rees M. J., 2006, MNRAS, 370, 289
 Bromm V., Loeb A., 2003, ApJ, 596, 34
 Chandrasekhar S., 1964, ApJ, 140, 417
 Clark P. C., Glover S. C. O., Klessen R. S., Bromm V., 2011, ApJ, 727, 110
 Coppola C. M., Longo S., Capitelli M., Palla F., Galli D., 2011, ApJS, 193, 7
 Dijkstra M., Haiman Z., Mesinger A., Wyithe J. S. B., 2008, MNRAS, 391, 1961
 Eisenstein D. J., Hu W., 1998, ApJ, 496, 605
 Fan X., 2006, New A Rev., 50, 665
 Fan X. et al., 2006, AJ, 131, 1203
 Fernandez R., Bryan G. L., Haiman Z., Li M., 2014, MNRAS, 439, 3798
 Field G. B., Somerville W. B., Dressler K., 1966, ARA&A, 4, 207
 Glover S., 2005, Space Sci. Rev., 117, 445
 Glover S. C. O., 2015, MNRAS, 451, 2082
 Glover S. C. O., 2016, arXiv:1610.05679
 Glover S. C. O., Abel T., 2008, MNRAS, 388, 1627
 Glover S. C. O., Jappsen A.-K., 2007, ApJ, 666, 1
 Greif T. H., White S. D. M., Klessen R. S., Springel V., 2011, ApJ, 736, 147
 Hahn O., Abel T., 2011, MNRAS, 415, 2101
 Hartwig T., Glover S. C. O., Klessen R. S., Latif M. A., Volonteri M., 2015, MNRAS, 452, 1233
 Hirano S., Hosokawa T., Yoshida N., Omukai K., Yorke H. W., 2015, MNRAS, 448, 568
 Hirata C. M., Padmanabhan N., 2006, MNRAS, 372, 1175
 Hosokawa T., Yorke H. W., Inayoshi K., Omukai K., Yoshida N., 2013, ApJ, 778, 178
 Inayoshi K., Omukai K., 2012, MNRAS, 422, 2539
 Inayoshi K., Tanaka T. L., 2015, MNRAS, 450, 4350
 Inayoshi K., Visbal E., Kashiyaama K., 2015, MNRAS, 453, 1692
 Latif M. A., Bovino S., Van Borm C., Grassi T., Schleicher D. R. G., Spaans M., 2014b, MNRAS, 443, 1979
 Latif M. A., Niemeyer J. C., Schleicher D. R. G., 2014, MNRAS, 440, 2969
 Latif M. A., Schleicher D. R. G., Bovino S., Grassi T., Spaans M., 2014a, ApJ, 792, 78
 Loeb A., Rasio F. A., 1994, ApJ, 432, 52
 Lupi A., Haardt F., Dotti M., Fiacconi D., Mayer L., Madau P., 2016, MNRAS, 456, 2993
 Machacek M. E., Bryan G. L., Abel T., 2001, ApJ, 548, 509
 Mocz P., Vogelsberger M., Pakmor R., Genel S., Springel V., Hernquist L., 2015, MNRAS, 452, 3853
 Mortlock D. J. et al., 2011, Nature, 474, 616
 Naoz S., Yoshida N., Gnedin N. Y., 2013, ApJ, 763, 27
 Oh S. P., Haiman Z., 2002, ApJ, 569, 558
 Pakmor R., Springel V., Bauer A., Mocz P., Munoz D. J., Ohlmann S. T., Schaal K., Zhu C., 2016, MNRAS, 455, 1134

- Pezzulli E., Valiante R., Schneider R., 2016, MNRAS, 458, 3047
- Planck Collaboration et al., 2016, A&A, 594, A13
- Regan J. A., Haehnelt M. G., 2009a, MNRAS, 396, 343
- Regan J. A., Haehnelt M. G., 2009b, MNRAS, 393, 858
- Regan J. A., Johansson P. H., Wise J. H., 2014, ApJ, 795, 137
- Regan J. A., Johansson P. H., Wise J. H., 2016a, MNRAS
- Regan J. A., Johansson P. H., Wise J. H., 2016b, MNRAS, 461, 111
- Regan J. A., Visbal E., Wise J. H., Haiman Z., Johansson P. H., Bryan G. L., 2017, Nature Astronomy, 1, 0075
- Sasaki M., Clark P. C., Springel V., Klessen R. S., Glover S. C. O., 2014, MNRAS, 442, 1942
- Schauer A. T. P. et al., 2017, MNRAS, 467, 2288
- Schauer A. T. P., Whalen D. J., Glover S. C. O., Klessen R. S., 2015, MNRAS, 454, 2441
- Schleicher D. R. G., Palla F., Ferrara A., Galli D., Latif M., 2013, A&A, 558, A59
- Shang C., Bryan G. L., Haiman Z., 2010, MNRAS, 402, 1249
- Springel V., 2010, MNRAS, 401, 791
- Stacy A., Bromm V., Loeb A., 2011, ApJ, 730, L1
- Stecher T. P., Williams D. A., 1967, ApJ, 149, L29
- Sugimura K., Omukai K., Inoue A. K., 2014, MNRAS, 445, 544
- Tanaka T. L., Li M., 2014, MNRAS, 439, 1092
- Tseliakhovich D., Hirata C., 2010, Phys. Rev. D, 82, 083520
- Visbal E., Haiman Z., Bryan G. L., 2014a, MNRAS, 442, L100
- Visbal E., Haiman Z., Bryan G. L., 2014b, MNRAS, 445, 1056
- Wu X.-B. et al., 2015, Nature, 518, 512
- Yoshida N., Abel T., Hernquist L., Sugiyama N., 2003, ApJ, 592, 645